Physicochemical Characterization of Morpholinium Cation Based Protic Ionic Liquids Used As Electrolytes

Catherine Brigouleix,[†] Mérièm Anouti,*,[†] Johan Jacquemin,[†] Magali Caillon-Caravanier,[†] Hervé Galiano,[‡] and Daniel Lemordant[†]

Université François Rabelais, Laboratoire PCMB (EA 4244), équipe de Chimie-physique des Interfaces et des Milieux Electrolytiques (CIME), Parc de Grandmont 37200 Tours, France, and CEA, LE RIPAULT, Laboratoire Synthèse et Transformation des Polymères, F-37260 Monts, France

New protic ionic liquids (PILs) based on the morpholinium, *N*-methylmorpholinium, and *N*-ethyl morpholinium cations have been synthesized through a simple and atom-economic neutralization reaction between *N*-alkyl morpholine and formic acid. Their densities, refractive indices, thermal properties, and electrochemical windows have been measured. The temperature dependence of their dynamic viscosity and ionic conductivity have also been determined. The results allow us to classify them according to a classical Walden diagram and to evaluate their "fragility". In addition, morpholinium based PILs exhibit a large electrochemical window as compared to other protic ionic liquids (up 2.91 V) and possess relatively high ionic conductivities of $10-16.8$ mS·cm^{-1} at 25 °C and $21-29$ mS·cm^{-1} at 100 °C, and a residual conductivity close to 1.0 mS·cm^{-1} at -15 °C. PIL−water mixtures exhibit high ionic conductivities up to 65 mS·cm^{-1} at 25 °C and 120 mS·cm^{-1} at 100 °C for morpholinium formate with water weight fraction $w_w = 0.6$. Morpholinium based PILs studied in this work have a low cost and low toxicity, are good ionic liquids, and prove extremely fragile. They have wide applicable perspectives as electrolytes for fuel cell devices, thermal transfer fluids, and acid-catalyzed reaction media as replacements of conventional solvents.

1. Introduction

Ionic liquids (ILs) are organic salts having melting points less than 100 °C. In recent years, they have received much attention due to their potential as alternative recyclable environmentally benign reaction media for chemical processes.[1–3]

ILs can be called "designer solvents" because their physical properties (such as melting point, viscosity, density, hydrophobicity, or hydrophilicity) can be modified according to the nature of the desired reactions by the modification of their cations and anions.[4] Key physical properties may be controlled by selection of appropriate cations and anions in the first instance, with fine-tuning facilitated by subtle variations in molecular structure.[4] The ability to carefully and predictably control physical properties has led to a vast number of papers concerning the use of ILs as solvents.[3,5–9]

Various new industrial applications of ILs have recently been considered owing to their unique electrochemical and physical properties.[10–17] In particular, a large number of ILs have been studied to promote the safety and performance of systems such as solar cells, fuel cells, capacitors, and lithium batteries. Among the advantages offered by ILs are low vapor pressure, negligible flammability, and high thermal stability. ILs with high ionic conductivity and electrochemical stability are potential candidates for use as electrolytes in batteries or supercapacitors.[18–22]

Most ILs are based on heterocyclic compounds, particularly the alkylimidazolium, alkyl pyrrolidinium, or alkylpyridinium cations. They can be broadly classified into two groups, protic and aprotic ILs.[23,24] Protic ionic liquids (PILs) are synthesized by proton transfer from a Brønsted acid to a Brønsted base, which creates proton donor and acceptor sites and can lead to the formation of hydrogen bonds.[25] Research concerning PILs has generally focused on surfactant self-assembly[26–32] and their physical properties.[23,24,33–36] There is presently much interest in proton-conducting electrolytes, due to their potential interest in many systems such as aqueous batteries, fuel cells, double-layer capacitors, dye sensitized solar cells, or actuators. PILs appear as promising materials for such applications. For instance, their ability to act as anhydrous proton conductors allows them to be associated with protonic membranes for proton exchange membrane fuel cells (PEMFCs). However, for such applications, they must satisfy stringent requirements, such as a high conductivity and satisfactory thermal and electrochemical stabilities.

Very recently, morpholinium based ILs received much attention because of their structural properties especially for the design of ionic liquid crystals.[37,38] There are also of interest as catalysts for organic synthesis,[39,40] heat stabilizers, or antioxidants for lubricating oils[41] and for electrochemical applications, for instance, as corrosion inhibitors.[42,43] They have been considered in recent inocuity tests, among other commonly used ILs.[44] In these works, the morpholinium cation is mainly associated to aprotic anions such as [BF$_4$]$^-$,[37,38] [TFSI]$^-$, [PF$_6$]$^-$, Br$^-$, anions with longer alkyl chains.[38,42] Only one article reports the association of morpholinium cation with a protic anion, [HSO$_4$]$^-$.[39] In spite of the interest of PILs, there is still limited information available on their physicochemical, thermodynamic, and electrochemical properties, of pure PILs or their mixtures with other fluids.
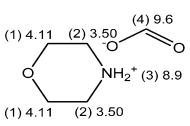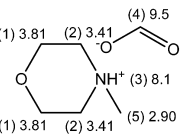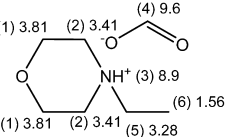
The present work reports the preparation of new PILs not thoroughly studied before, namely, morpholinium formate, *N*-methylmorpholinium formate, and *N*-ethylmorpholinium for-

* To whom correspondence should be addressed. E-mail: meriem.anouti@univ-tours.fr. Fax: (33)247367360. Telephone: (33)247366951.
† Université François Rabelais.
‡ CEA, LE RIPAULT.

TABLE 1: Names, Abbreviations, Structures, and ¹H NMR Spectrum Characteristics of Selected PILs

Protic Ionic Liquid Name and Abbreviation	PILs structure and δ in ppm	¹H-NMR characteristics
morpholinium formate [morph][F]	(1) 4.11 (2) 3.50 (4) 9.6 O NH₂⁺ (3) 8.9 (1) 4.11 (2) 3.50	(1) t, 4H (2) t, 4H (3) s, 2H (4) s, 1H
N-methylmorpholinium formate [Mmorph][F]	(1) 3.81 (2) 3.41 (4) 9.5 O NH⁺ (3) 8.1 (1) 3.81 (2) 3.41 (5) 2.90	(1) t, 4H (2) t, 4H (3) s, 2H (4) s, 1H (5) s, 3H
N-ethylmorpholinium formate [Emorph][F]	(1) 3.81 (2) 3.41 (4) 9.6 O NH⁺ (3) 8.9 (6) 1.56 (1) 3.81 (2) 3.41 (5) 3.28	(1) t, 4H (4) s, 1H (2) b.s, 4H (5) b.s, 2H (3) s, 2H (6) t, 3H

* b.s : broad signal

mate, denoted [morph][F], [Mmorph][F], and [Emorph][F], respectively. It is a continuation of our previous studies of PILs including the formate anion associated with pyrrolidinium and diisopropyl-ethylammonium cations.[45–47] Very few data are available on present PILs. Morpholinium formate has been mentioned as a solvent for the synthesis of purine base-8-13C but with no details about its physicochemical properties.[48] No data are available about [Mmorph][F] and [Emorph][F]. The present article reports the physicochemical properties of these PILs and their dependence on the nature of the substituent in the cation. The temperature behavior of the dynamic viscosity, the ionic conductivity, and the phase behavior of these PILs have been measured and investigated in detail. The results allow us to classify them according to a classical Walden diagram and to evaluate their ionicity and their "fragility". Finally, their electrochemical stabilities were measured by using carbon graphite as electrode material. The results obtained are compared with pyrrolidinium based PILs and discussed in relation to the geometric and electrostatic parameters on ions.

2. Experimental Section

2.1. Materials. Morpholine, *N*-methyl morpholine, and *N*-ethyl morpholine are commercially available from Fluka (>99.0%) and are used without further purification. The formic acid (>99.0%) is obtained from Sigma Aldrich. Water is purified with a Milli-Q 18.3 MΩ water system.
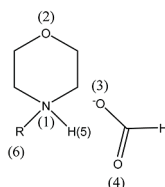
2.2. Preparation of PILs. *N*-Alkylmorpholinium based ILs are obtained as the products of an equimolar reaction between formic acid and correspondent bases. Amine is introduced in a three-neck round-bottom flask immerged in an ice bath and equipped with a reflux condenser, a dropping funnel to add the acid, and a thermometer to monitor the temperature. Under vigorous stirring, formic acid is added dropwise to the amine (60 min). As this acid−base reaction is exothermic, the mixture temperature is maintained below 25 °C during the addition of the acid by use of the ice bath. Stirring is maintained for 4 h at ambient temperature. The residual amine or acid is evaporated under reduced pressure, and the remaining liquid is further dried at 80 °C under reduced pressure (1−5 mmHg) to obtain the target PILs (yield > 98.7%). [Mmorph][F] and [Emorph][F] are liquid at ambient temperature. [morph][F] is obtained as white

crystals having a melting point close to 50 °C and can be maintained in subcooled state at 25 °C. Names, structures, and abbreviations of studied PILs are reported in Table 1. The water content, measured by the Karl Fischer titration method, is between 50 and 100 ppm. ¹H NMR spectra (200 MHz, CDCl₃, TMS) of these PILs show that the protons resonate in the δ ranges summarized in Table 1. As a volume of PIL is poured into D₂O, only the signal due to the hydrogen carried by the nitrogen disappears. This indicates that this is the only labile proton.

2.3. Measurements. Measurements of refractive index are achieved at 25 °C with an ABBE refractive index instrument, calibrated with deionized water. Densities are determined by the weight method at 25 °C. Viscosities are measured using a TA Instruments rheometer (AR 1000) with conical geometry as a function of temperature (from 25 to 80 °C). Ionic conductivities are measured by using a Crison (GLP 31) digital multifrequencies conductimeter. The temperature control (from −5 to 120 °C) is ensured by a JULABO thermostated bath. PILs' electrochemical windows are checked by linear voltammetry using an EGG M 270A electrochemical workstation and a three-electrode configuration. A 3 mm diameter vitreous carbon disk is used as working electrode, a platinum wire as counter electrode, and an $Ag/AgCl_{sat}, KCl_{sat(PIL)}$ electrode as reference. The reference $Ag/AgCl_{sat}, KCl_{sat(PIL)}$ system is calibrated versus the SHE electrode using the ferrocenium ion/ferrocene couple: $E_{ref} = -0.150$ V/SHE. (The calculation is specified as follows: The reference electrode has been prepared by filling an Ag/AgCl electrode with a room temperature protic ionic liquid such as pyrrolidinium formate saturated with KCl and AgCl. The ferrocenium ion/ferrocene couple is used to calibrate the reference electrode by using $E(Ag/AgCl_{AgClsat.(PIL),KClsat.(PIL)})/SHE = E_{Fc}^{0/+}/SHE - E_{Fc}^{0/+}/Ag/AgCl_{AgClsat.(PIL),KClsat.(PIL)}$. The numerical application gives $E(Ag/AgCl_{AgClsat.(PIL),KClsat.(PIL)})/SHE = 0.45 - 0.60 = -0.15$ V/SHE.) The influence of possible reactions between ferrocenium cations and formate anions is evaluated as detailed in the electrochemical section. The potential windows of all PILs have been measured by cyclic voltammetry at a scan rate of 50 mV·s⁻¹ at 25 °C for [Mmorph][F] and [Emorph][F] and at 60 °C for [morph][F]. Differential scanning calorimetry (DSC) is carried out on a

Morpholinium Based Protic Ionic Liquids

J. Phys. Chem. B, Vol. 114, No. 5, 2010 **1759**

TABLE 2: Total Charge Density of Molecular Orbital, Length of H-Bond (pm), and Partial Charge on Some Atoms in Cation and Anion

PIL Structure	[morph][F]		[Mmorph][F]		[Emorph][F]	
Total charge density of molecular orbital Atom color by partial charge Dashed line : H-bond						
Length H-bond (pm)	H(5)-O(3)	177.71	H(5)-O(3)	164.48	H(5)-O(3)	160.96
	H(6)-O(3)	178.17	H(5)-O(4)	200.70		
	H(5)-O(4)	193.01				
Partial charge δ'	N 0.405 [N(1)]		N 0.643 [N(1)]		N 0.466 [N(1)]	
	O -0.362 [O(2)]		O -0.362 [O(2)]		O -0.358 [O(2)]	
	O -0.636 [O(3)]		O -0.707 [O(3)]		O -0.656 [O(3)]	
	O -0.672 [O(4)]		O -0.740 [O(4)]		O -0.637 [O(4)]	
	H 0.182 [H(5)]		H 0.142 [H(5)]		H 0.175 [H(5)]	
	H 0.103 [H(6)] (R = H)					

TABLE 3: Refractive Index, Difference in pK_a of Reagents, Density, Molar Volume, Viscosity, and Specific and Equivalent Ionic Conductivity of PILs

PIL	$n_D \pm 0.05\%$	ΔpK_a	$\rho \pm 0.1\%$ (g·cm^{-3})	$V_m \pm 0.1\%$ (cm^3·mol^{-1})	$\eta \pm 0.1\%$ (cP)	$\sigma \pm 2\%$ (mS·cm^{-1})[b]	$\Lambda \pm 2\%$ (S·cm^2·mol^{-1})[b]
[morph][F]	1.4707[a]	4.61	1.155[a]	115.3[a]	21.20[a]	9.92	1.14
[Mmorph][F]	1.4517	3.66	1.126	130.7	5.86	16.77	2.19
[Emorph][F]	1.4535	3.95	1.062	151.8	10.64	12.17	1.85

[a] Subcooled state. [b] Measured at 60 °C.

Perkin-Elmer DSC6 instrument under N_2 atmosphere. Samples for DSC measurements are sealed in aluminum pans. Thermograms are recorded from −120 to 400 °C with a scan rate of 5 °C·min^{-1}.

3. Results and Characterizations

3.1. Theoretical Study of the PIL Structures. To understand the interactions between cation and anion in PILs, the geometries of all studied structures were determined by complete geometry optimizations with the GAMESS interface using restricted Hartree−Fock (RHF) calculations with the split-valence 3-21G basis set. In Table 2, the obtained geometries are represented within the total electron density. Mulliken atomic charges and H-bond distances for the more stable PIL conformers are shown in Table 2.

It appears that [morph][F], [Mmorph][F], and [Emorph][F] present three, two, and one H-bonds between anion and cation, respectively. On the other hand, the partial charges are more localized on the nitrogen atom (δ'_N) of the cation and oxygen atoms (δ'_O) of the formate anion in the case of [Mmorph][F] by comparison with the two other studied PILs (Table 2). Indeed, $\delta'_N = +0.405$ for [morph][F], $\delta'_N = +0.643$ for [Mmorph][F], and $\delta'_N = +0.466$ for [Emorph][F]. In other words, hydrogen bond interactions between cations and anions are stronger and allow a better charge distribution for the [morph][F] and [Emorph][F].

3.2. Physical Properties of PILs. Physicochemical properties of studied PILs are shown in Table 3.

Refractive Index. The refractive index n_D is related to the polarizability/dipolarity of the environment and can provide useful information when studying the interaction forces between molecules.[49] Greaves et al. reported an increase of this property from 1.41 to 1.47 on going from 1 to 4 labile protons and increase with the length of alkyl chains.[50] It is noted that refractive index is proportional to free volume; it evolves in the opposite direction of the PIL molar volumes (Table 3). Indeed, the morpholinium formate has the lesser molar volume and the higher n_D.

Density. The density of ionic liquids falls typically in the range from 1.2 to 1.6 g·cm^{-3}.[51] In general, the density of aprotic ionic liquids is very strongly affected by the nature of the anion. For example, at 25 °C, densities of 1-butyl-3-methylimidazolium are equal to 1.2023, 1.3673, 1.2170, and 1.4366 g·cm^{-3} with [BF$_4$]$^-$, [PF$_6$]$^-$, [TFA]$^-$, and [TFSI]$^-$ anions, respectively.[52−55] In the case of PILs, the nature of the anion has also a large impact on density. For example, pyrrolidinium based salts show larger densities with mineral counteranion (1.1675 and 1.3421 g·cm^{-3} for [NO$_3$]$^-$ and [HSO$_4$$^-$], respectively) than those constituted with organic anion (0.9485, 1.0543, and 1.1190 g·cm^{-3} for [C$_7$H$_{15}$COO]$^-$, [CH$_3$COO]$^-$, and [HCOO]$^-$, respectively).[47] For the PILs studied in this paper, densities are related to the compactness of their structures. When the alkyl chain length increases, the density decreases: $\rho = 1.153$ g·cm^{-3} for [morph][F], $\rho = 1.126$ g·cm^{-3} for [Mmorph][F], and $\rho = 1.062$ g·cm^{-3} for [Emorph][F] as reported in Table 3.

Viscosity. The viscosity is a very important parameter in electrochemical studies due to its strong effect on the rate of mass transport within solution. For PILs, the relative significance of van der Waals interactions increases as one of the ions exhibits longer alkyl chains or a higher degree of branching.[20]
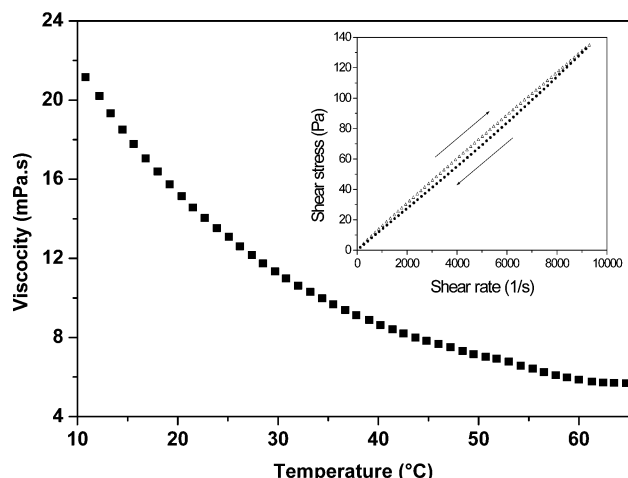
Figure 1. Evolution of the viscosity of [Mmorph][F]. Inset: shear stress versus shear rate at 25 °C.

Generally, ionic liquids are more viscous than common molecular solvents. Indeed, while the viscosity of water, for instance, is only 0.8903 cP at 25 °C, viscosities of ILs typically range from 30 to 100 cP at room temperature, and can reach values as high as 1000 cP in some cases.[50,56] The identities of the anion and the cation which compose the ionic liquid have a huge effect on the viscosity of the ionic liquid. With respect to the anionic species, higher basicity, size, and relative capacity to form hydrogen bonds result in more viscous ILs. Due to the acid/base character of PILs, their viscosity depends dramatically on hydrogen bonds. Thus, aprotic ionic liquids containing $[PF_6]^-$ anion are much more viscous (1-ethyl-2-methylimidazolium PF_6, $\eta > 1000$ cP) than those formed with $[TFSI]^-$ anion (1-ethyl-2-methylimidazolium TFSI $\eta = 69$ cP), where the negative charge is more delocalized.[56] Moreover, IL viscosities appear to be ruled also by van der Waals interactions[57] and cationic size.[58] The viscosities of presently studied PILs are 21.20, 5.86, and 10.64 cP for [morph][F], [Mmorph][F], and [Emorph][F], respectively. The largest viscosity compared for two other PILs has been measured for [Morph][F], for which labile protons may be involved in a number of hydrogen bonds as illustrated in Table 2. The lower steric hindrance of the nonsubstituted morpholinium ring with alkyl chain increases its ability to accept hydrogen bonds. On the other hand, the viscosity decreases on going from [Emorph][F] to [Mmorph][F], as expected on the basis of the respective alkyl chain lengths.

Figure 1 exhibits the temperature dependence of viscosity data for [Mmorph][F]. The viscosity decreases as the temperature is raised from 25 to 60 °C owing to the higher mobility of the ions. In this temperature range, they exhibit a Newtonian behavior. Indeed, shear stress versus shear rate is linear as reported in the inset in Figure 1 for [Mmorph][F].

PIL viscosities typically exhibit non-Arrhenius behavior, that is, a distinct downward curvature at lower temperatures in the Arrhenius plot. Viscosity data can be fitted to the Vogel−Tamman−Fulcher (VTF) equation.

$$\eta = \eta_0 \exp\left[\frac{B}{(T - T_0)}\right] \qquad (1)$$

where η_0 (cP), B (K), and T_0 (K) are fitting parameters. The product BR (R is the molar gas constant) has the dimension of activation energy (kJ·mol^{-1}). Experimental data are then fitted by using eq 1, where T_0 is taken equal to the glass transition

TABLE 4: VTF Equation Parameters for Viscosity (η_0, B, T_0) (eq 1)

IL	η_0 (cP)	$T_0 = T_g$ (K)	B (K)[a]	R^{2b}
[morph][F]	0.25	186	636.8	0.9936
[Mmorph][F]	0.43	184	389.0	0.9996
[Emorph][F]	0.33	184	464.5	0.9979

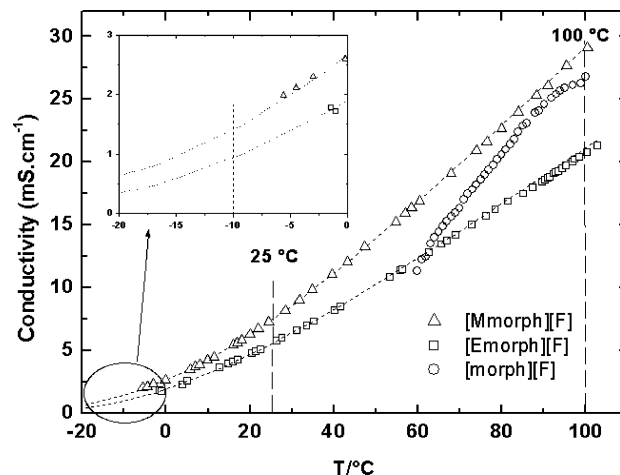[a] $BR \equiv$ activation energy (kJ·mol^{-1}). [b] Squared correlation coefficient.

Figure 2. Influence of temperature on conductivity for PILs of this study.

temperature (T_g) for each compound, determined by DSC (presented in the Thermal Properties subsection). The best-fit parameters η_0, B and the associated squared correlation coefficients R^2 are given in Table 4.

Conductivity. For any electrochemical process, the conductivity knowledge is essential. Being composed entirely of ions, ILs are supposed to be among the most concentrated electrolytic fluids with many charge carriers per unit volume. When these charge carriers are mobile, very high conductivities are possible. Ionic liquids have reasonably good ionic conductivities compared to those of organic solvent/electrolyte systems (up to 10 mS·cm^{-1}).[59] However, at room temperature, their conductivities are usually lower than those of concentrated aqueous electrolytes. PIL conductivities are higher than those of aprotic ILs.[50]

At 25 °C, the conductivity values of [Mmorph][F] and [Emorph][F] are 7.41 and 5.63 mS·cm^{-1}, respectively. At 60 °C, the conductivities of [morph][F], [Mmorph][F], and [Emorph][F] are 9.92, 16.77, and 12.17 mS·cm^{-1}, respectively (Table 3). Its appears that [Mmorph][F], which presents lower viscosity (Table 3) and charge density of the surface (Table 2), has higher conductivity.

Present conductivity values are comparable to most values reported earlier for PILs, based on either the alkylammonium cation (diisopropyl-methylammonium formate, $\sigma = 8.2$ mS·cm^{-1} [45]), on the imidazolium cation (1-methylimidazolium formate, $\sigma = 20$ mS·cm^{-1} [60]), or on the pyrrolidinium cation (pyrrolidinium formate, $\sigma = 32.9$ mS·cm^{-1} [61]).

The temperature dependence of the ionic conductivity for [Mmorph][F] and [Emorph][F] is shown in Figure 2. As expected, conductivities increase with temperature, up to 29 mS·cm^{-1} at 100 °C in the case of [Mmorph][F]. Moreover, these PILs present residual conductivities at −15 °C close to 0.5 and 1.0 mS·cm^{-1} for [Emorph][F] and [Mmorph][F], respectively. This opens promising perspectives for low temperature applications of this family of PILs based on the morpholinium cation as a new electrolyte.
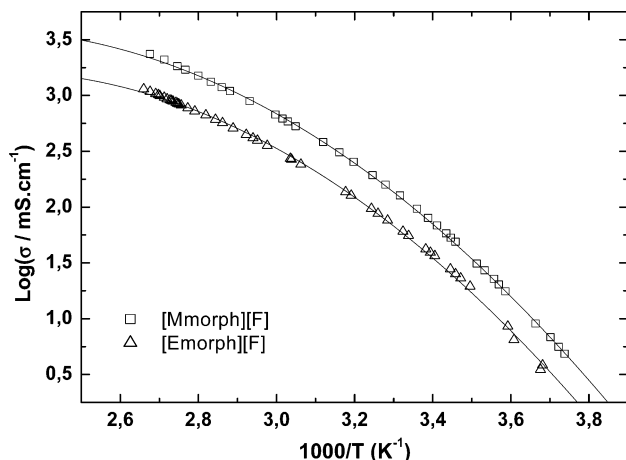
Morpholinium Based Protic Ionic Liquids

J. Phys. Chem. B, Vol. 114, No. 5, 2010 **1761**

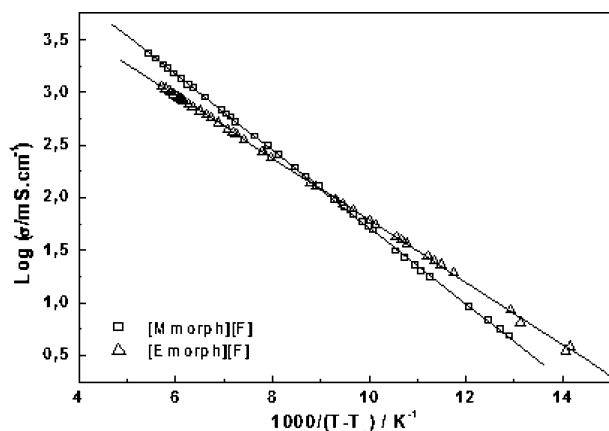**Figure 3.** Arrhenius plot for [Mmorph][F] and [Emorph][F].

Figure 4. VTF plot of ionic conductivities for selected PILs. The line represents the VTF fittings with the parameters indicated in Table 5.

TABLE 5: VTF Equation Parameters for Ion Conductivity (σ_0, B', T_0)

IL	$T_0 = T_g$ (K)	σ_0 (S·cm^{-1})	B' (K)	R^{2a}
[morph][F]	186	453	519	0.986
[Mmorph][F]	184	249	403	0.999
[Emorph][F]	184	170	395	0.998

[a] Correlation coefficient.

As expected from viscosity results, PIL conductivities exhibit non-Arrhenius behavior as shown in Figure 3. Therefore, the Vogel−Tammann−Fulcher (VTF) eq 2 is used to represent the temperature dependence of the conductivity.

$$\sigma = \sigma_0 \exp\left[\frac{-B'}{(T - T_0)}\right] \qquad (2)$$

For example, in Figure 4, variations of $\ln(\sigma)$ versus $1/(T - T_0)$ for [Mmorph][F] and [Emorph][F] are plotted. The best-fit values for σ_0 (S·cm^{-1}), B' (K), and T_0 (K) parameters are given in Table 6.

Effect of Water on the Conductivity and Viscosity. PILs provide a new opportunity for studying the conductivity of protic electrolyte solutions in salt-rich regions. Many molecular solvents are miscible with PILs, which allows us to investigate the dependence of the ionic conductivity on the property of PILs and some solvent, particularly the water. The ionic conductivities for aqueous mixtures of [morph][F], [Mmorph][F], and [Emor-
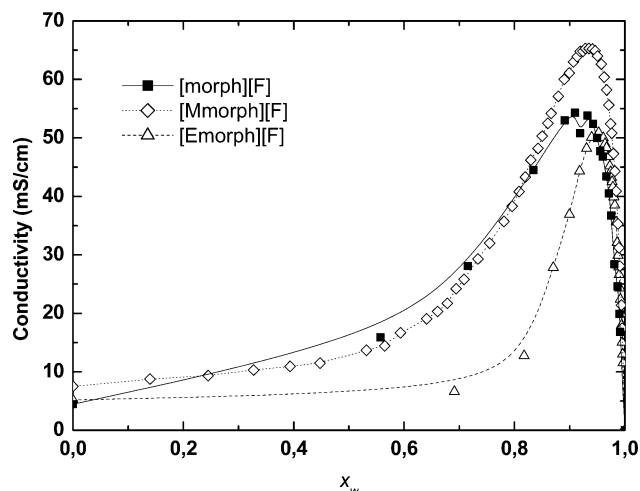

Figure 5. Evolution of the conductivity as a function of the molar fraction of water added for PILs of this study at 25 °C.

ph][F] versus water mole fraction x_w are reported in Figure 5. They present a maximum at $x_w = 0.9$, corresponding to a 5-fold enhancement of the values for pure ILs. This variation is due to two phenomena: the destruction of the PIL structure by incorporation of water and the reorganization of the binary system (PIL + water). The solvation of ions by water increases their mobility and the conductivity of the binary system by comparison with the case of pure PILs. Below $x_w = 0.9$, the dilution effect becomes predominant and solution conductivity decreases down to the water conductivity.

Increasing the temperature from 25 to 60 °C leads to a significant enhancement of the conductivity. For example, the conductivity value at 60 °C can reach 120 mS·cm^{-1} for water weight fraction $w_w = 0.6$ for the [morph][F] + water system as shown in Figure 6a. Moreover, the position of the maximum is not modified significantly which suggests that the ion solvation shell is not affected. The variation of viscosity of aqueous solution of morpholinium formate as a function of the water weight fraction is presented in Figure 6b. We observe that the viscosity decreases with the weight fraction of water in the mixture. In the case of [morph][F], $\eta = 21.20$ and 2.40 mPa·s for $w_w = 0$ and 0.6, respectively.

To understand the relation between the conductivity and the viscosity of aqueous solutions of PILs, experimental conductivities are converted into specific conductivities ($\Lambda = \sigma/C$). The Walden product, $\Lambda\eta$, is then plotted versus the water weight fraction as shown in Figure 6c. We note, in this figure, that $\Lambda\eta$ is not constant. In other words, the ionic conductivity increase is not only caused by the decrease of viscosity when the water is added. Indeed, in the PIL−water mixture, the aggregates must be formed by establishing H-bonds, and in fact the Walden product changes with the composition.

Furthermore, Λ is plotted versus the square of the concentration of PILs according to Kohlraush's equation: $\Lambda = \Lambda_\infty - b\sqrt{C}$, where Λ_∞ is the molar conductivity at infinite dilution and b is an empirical constant. The plot of Λ versus $\sqrt{C}$ for the present PILs is shown in Figure 7. The molar conductivities at infinite dilution Λ_∞ were determined by extrapolating the Λ values in the low concentration regime to infinite dilution. As Λ_∞ is the sum of the molar conductivities of cation and anion at infinite dilution (Kohlraush law), that is, $\Lambda_\infty = \Lambda_\infty([cation]^+) + \Lambda_\infty([F]^-)$, at $T = 298$ K.

The extrapolated values are $\Lambda_\infty = 49.7$, 80.9, and 77.9 S·cm^2·mol^{-1} for [morph][F], [Mmorph][F], and [Emorph][F],
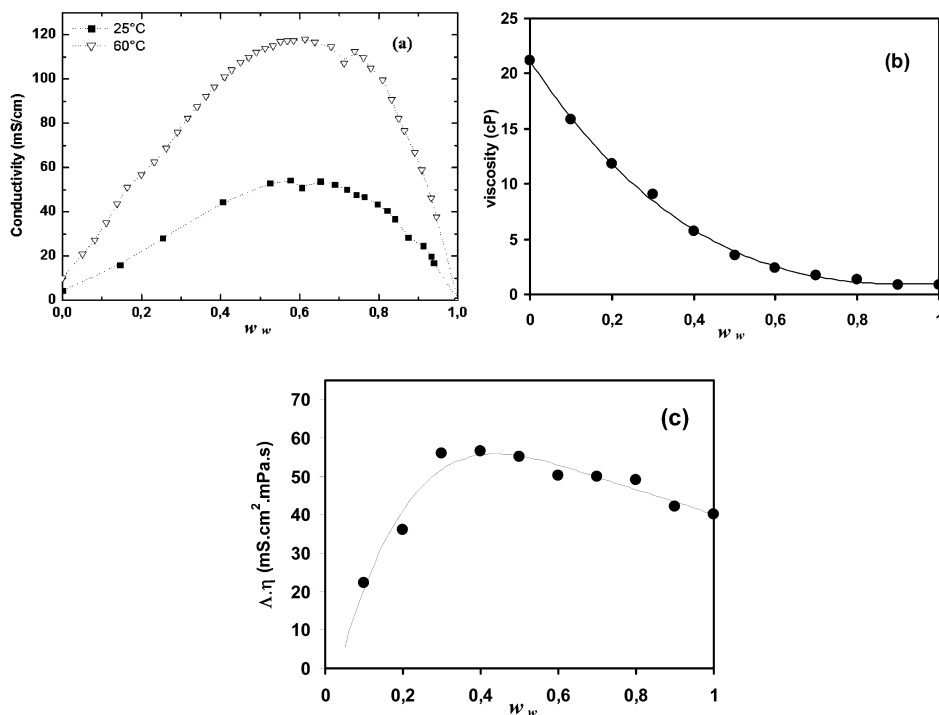
Figure 6. Evolution of the conductivity at 25 and 60 °C (a), of the viscosity at 25 °C (b), and of the Walden product (c) of [morph][F] as a function of the water weight fraction, w_w.
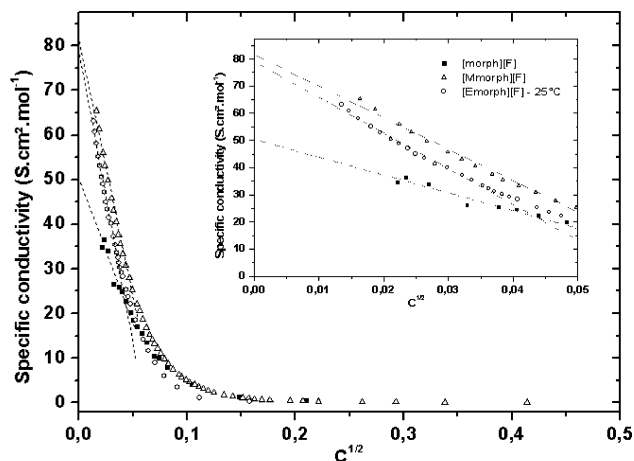

Figure 7. Determination of the specific conductivity at infinite dilution for the three PILs of this study at 25 °C. The values are extrapolated from the linear part for $c^{1/2}$ below 0.04 $mol^{1/2} \cdot L^{-1/2}$.

respectively. They reflect the relative cations mobilities. Indeed, the [morph]$^+$ ion is more solvated and hence less mobile than the two other cations. Using Stoke's law and the definition of the ion mobility, we can express the ion mobility in term of the viscosity of the medium and also in terms of the radius r_i of the ion in the solution (by considering this ion as a hard sphere).[62] The mobility of ions is related to its strong tendency to establish hydrogen bonds with water shown in Table 2.

3.3. Electrochemical Stability. Electrolytes for electrochemical devices should resist reduction and oxidation and exhibit a large electrochemical window. Typical windows of 4.5−5 V have been reported for aprotic ILs,[61] equivalent to the observed potential window range in conventional organic electrolytes. For PILs, few potential window data are mentioned in literature except for the PIL family containing alkylammonium cation. For these PILs, a electrochemical window range of 1.3 V < ΔE < 4.3 V is reported in the literature; nevertheless, these PILs present also high viscosities (η = 336 cP for

diethanolammonium acetate) and low conductivities (σ = 0.14 mS·cm^{-1} for diethanolammonium acetate).[63] The electrochemical stabilities of PILs studied in this work were measured at room temperature using a vitreous carbon working electrode and Ag/AgCl$_{sat}$, KCl$_{sat(PIL)}$ reference electrode. In order to compare obtained voltammetric data with literature, it is necessary to use a reference system with a known potential against a standard reference electrode. Furthermore, the reference potential system must be independent to the nature of the ionic liquid. The ferrocene/ferrocenium couple is most commonly used as an internal potential scale standard in voltammetry in traditional organic solvent medium containing an electrolyte.[64,65] The reference Ag/AgCl$_{sat}$, KCl$_{sat(PIL)}$ system used as reference electrode is calibrated versus the SHE electrode using the ferrocenium ion/ferrocene couple: E_{ref} = −0.150 mV/SHE. The possible reaction of ferrocenium cations with formate anions in PILs for scan rates <0.2 V·s^{-1} has been already discussed.[63] The voltammogram with the ferrocenium/ferrocene couple (Figure 8) exhibits a peak-to-peak potential separation (ΔEp) of 90.8 mV and a peak current ratio |$i_{p,c}/i_{p,a}$| = 1.15. This indicates a quasi-reversible behavior, allowing the assessment of the electrochemical windows.[66]

In this work, electrochemical windows are defined as the potential range where the limiting current density reaches 1.0 mA·cm^{-2}. Voltammograms reported in Figure 8 show that the stability window ranges for studied PILs from 2.18 to 2.90 V/SHE. These values are similar to those found previously for diisopropyl-alkyl-ammonium formate (ΔV = 2.70 V).[45] They largely exceed the values observed for aqueous electrolytes. Reduction and oxidation potential limits are reported with respect to SHE in Table 6. In Figure 8, a small wave at E = −0.8 V may be noted for [Emorph][F], which could be assigned to the reduction of water. It is probably due to free water (<500 ppm) in the media. This wave is not observed in the cases of [morph][F] and [Mmorph][F].

It has been shown that the oxidation of the anions and the reduction of the cations, respectively, are responsible for the
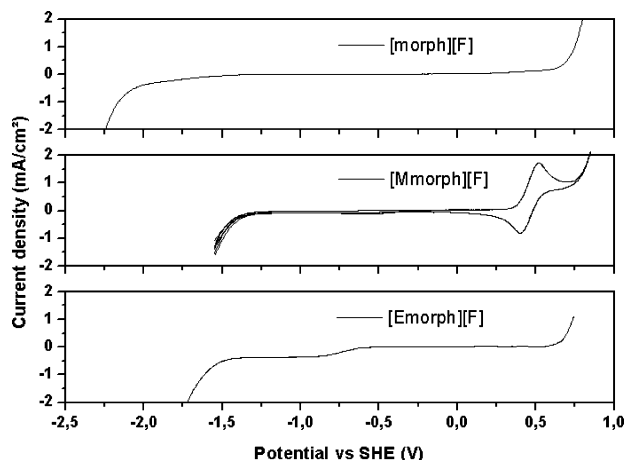
Morpholinium Based Protic Ionic Liquids

J. Phys. Chem. B, Vol. 114, No. 5, 2010 **1763**

Figure 8. Cyclic voltamograms ($v = 50$ mV·s^{-1}) obtained with a vitreous carbon working electrode for studied PILs. The ferrocenium/ferrocene couple has been added with [Mmorph][F] in order to calibrate the reference electrode.

TABLE 6: Electrochemical Potential Windows (ΔV) and Anodic and Cathodic Limit (V) versus SHE at 25°C

ILs	potential windows (ΔV)	anodic limit (V)[a]	cathodic limit (V)[a]
[morph][F]	2.91	0.74	−2.16
[Mmorph][F]	2.18	0.84	−1.33
[Emorph][F]	2.33	0.76	−1.56

[a] Defined as the potential redox when the current density (J) is 1 mA·cm^{-2}.

anodic and cathodic limits observed in the ionic liquids.[67–69] The mechanisms presently assumed for these reactions rely on an analogy with results in organic media. They remain to be confirmed in IL media. According to these mechanisms, the formate anion is oxidized at relatively low potential at 0.75 V versus SHE:[70]
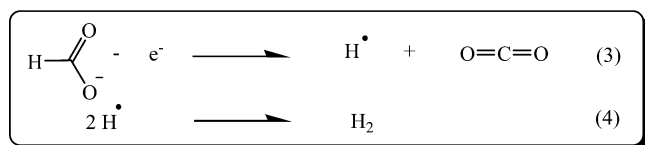
The Kolbe reaction (eqs 3 and 4) involves the formation of H_2 and CO_2. The reduction of morpholinium cation proceeds by CE mechanism. The deprotonation of morpholinium cation (eq 5) first occurs. It is followed by the reduction of proton (eq 6):
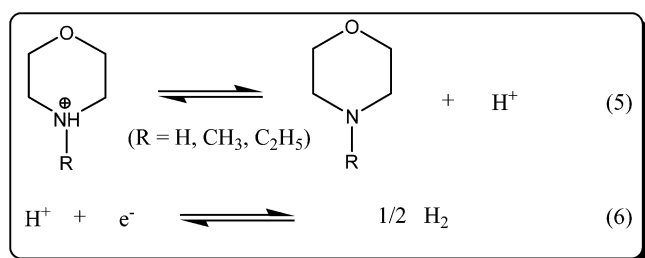

Figure 8 shows that the morpholinium cation is reducible at a variable potential according to the nature of the attached substituent on the nitrogen atom: $E_{red} = -2.2$, -1.6, and -1.2

V versus SHE reference for [morph][F], [Emorph][F], and [Mmorph][F], respectively. The [morph]$^+$ cation is stabilized by its increased ability to accept hydrogen bonds (Table 2). The equilibrium (eq 5) is then displaced toward the protonated cation. The reduction of the *N*-alkyl substituted morpholinium cation is related to the "high" acidity of the N−H proton (eq 5). Accordingly, [morph][F] exhibits a weaker acidity, giving a more negative reduction potential.

3.4. Thermal Properties. The thermal behavior of studied PILs is investigated by DSC from −120 to 400 °C. Figure 9 reports a thermogram showing different phase transitions observed at subambient temperatures from −120 to 20 °C for [morph][F]. The characteristic temperatures determined from the maximum of the respective peaks are listed in Table 7. The sample, first quenched in liquid nitrogen, undergoes a heating step (A) leading to a vitreous phase. The glass transition (T_g) occurs at 186 K. Then a broad devitrification peak ([1] in Figure 9) ($T_c = 245$ K) with a shoulder ($T_e = 233$ K) is observed. The shoulder is attributed to the crystallization of the eutectic formed between the PIL and a trace of acid or morpholine residual. A second peak ([2] in Figure 9) corresponds to the devitrification of the PIL ($T_m = 278$ K). This behavior is similar to that observed for [Im][TFSI] in variable proportions around equimolar composition.[71] A second cycle, cooling step (B) and heating step (C), induces a recrystallization peak ([3] in Figure 9) at 253 K, followed by a fusion peak ([4] in Figure 9) at $T_m = 280$ K. No glass transition is observed on reheating the sample cycle (C).

As presented in Figure 10, both [Mmorph][F] and [Emorph][F] exhibit a similar thermal behavior at subambient temperature, with a glass transition at 184 K. [Mmorph][F] does not present crystallization or fusion peaks in the studied temperature range. On the other hand, [Emorph][F] presents a crystallization peak at $T_c = 241$ K and a melting point at $T_m = 251$ K. Fusion and crystallization enthalpies have been then calculated from each peak area and listed in Table 7. No difference is observed between the T_g values of the three PILs. In fact, T_g is not affected by the nature of the substituent attached on the nitrogen atom of the morpholinium ring, in contrast to the crystallization and melting temperatures.

DSC measurements were then carried out from 20 to 400 °C for the three PILs (Figure 11). Each studied PIL exhibits vaporization peaks, T_b, at 410 K. No decomposition is observed below 673 K.
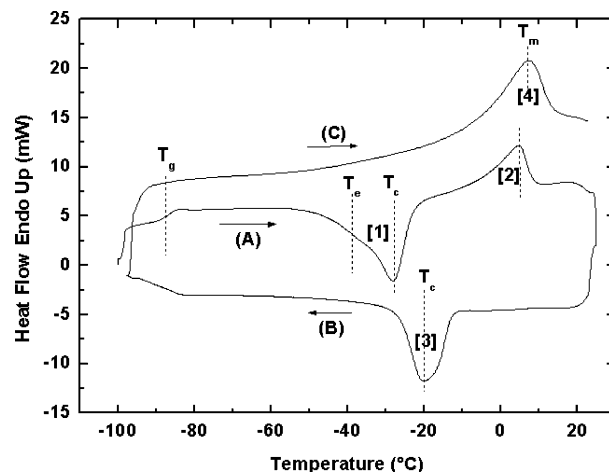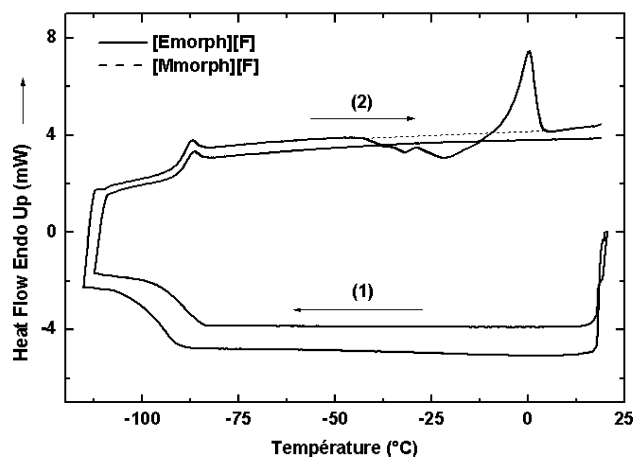

Figure 9. DSC thermogram showing the different phase transitions of [morph][F]. After quenching, the sample is heated (A), then cooled (B), and finally heated again (C). Each peak is associated with a number. The corresponding thermodynamic data are reported in Table 7.

TABLE 7: PIL Thermal Properties: Glass Transition (T_g), Eutectic (T_e), Devitrification (T_c), Melting Point (T_m), Boiling Point (T_b), Decomposition Point (T_d), Isobaric Heat Capacity (C_p/J·K^{-1}·g^{-1}), Heat Storage Density (D_h/MJ·m^{-3}), Crystallization Enthalpy (ΔH_c/kJ·mol^{-1}), and Melting Enthalpy (ΔH_m/kJ·mol^{-1})[a]

PIL	T_g	T_e	T_c	T_m	T_b	T_d	C_p[b]	D_h[c]	ΔH_c	ΔH_m
[Morph][F]	186	233 [1]	245 [1]	278 [2]	425	>673	0.76	90	−13.98 [1]	4.75 [2]
			253 [3]	280 [4]	411	>673			−8.87 [3]	14.43 [4]
[Mmorph][F]	184		−	−	409	>673	3.38	380	−	−
[Emorph][F]	184		241	251			1.52	165	−2.71	3.05

[a] All temperatures are in K. [b] Values at 30 °C. [c] $D_h = \rho C_p \Delta T$, with $\Delta T = 100$ °C. [X] is the number of the corresponding peak in Figure 9.

Figure 10. DSC thermograms showing the different phase transitions of [Mmorph][F] and [Emorph][F]. First, the sample is cooled (1) and then reheated (2).
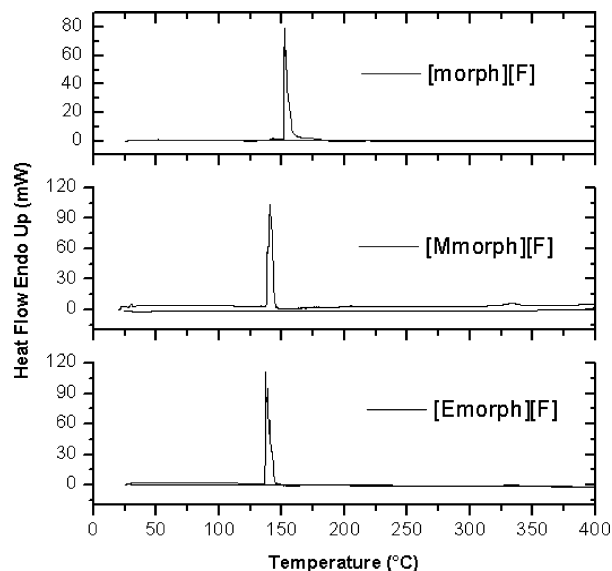
Figure 11. DSC thermograms recorded with a scan rate of 5 °C·min^{-1} for PILs of this study.

The isobaric heat capacity of ILs is an important feature of liquids which could be used as thermofluids. This property and the respective value of heat storage density are reported in Table 7. The heat capacity of [Emorph][F] ($C_p = 1.52$ J·g^{-1}·K^{-1}) has the same order of magnitude reported for aprotic ILs, such as [BMIm][BF$_4$] (1.63 J·g^{-1}·K^{-1}),[72] whereas [morph][F] and [Mmorph][F] exhibit lower values $C_p = 0.76$ and 3.38 J·g^{-1}·K^{-1}, respectively. Moreover, present morpholinium based PILs have larger heat storage densities, D_h, ranging from 86 to 166 MJ·m^{-3}. All values are much higher than the minimum storage density (1.9 MJ·m^{-3}) specified by the American National Renewable Energy Laboratory.[72] These PILs are therefore of potential interest as heat-transfer fluids.
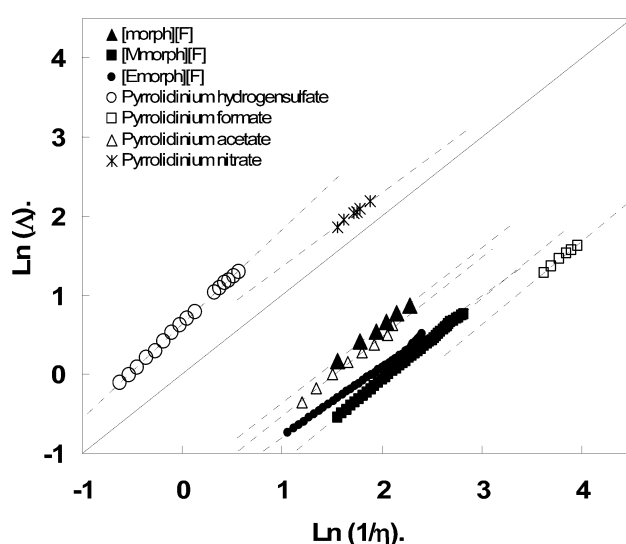
Figure 12. Walden plots for present PILs and comparison with literature results (open symbols).[47]

3.5. Ionicity and "Fragility" of Studied PILs. *Ionicity.* One way of assessing the ionicity of ionic liquids is to use the classification diagram based on the classical Walden rule.[73] This rule relates the ionic mobilities represented by the equivalent conductivity Λ to the fluidity η of the medium through which the ions move.[74,75] Λ is obtained as $V_m \sigma$, where V_m is the molar volume. Figure 12 shows the variation of $\ln(\Lambda)$ versus $\ln(1/\eta)$ at various temperatures for selected PILs. The ideal line is obtained for ionic mobilities determined only by the viscosity of the medium.[50] Its position is established by using aqueous KCl solutions at high dilution. The ionicity rule of studied PILs is presented and then compared with already available data from the literature for pyrrolidinium based PILs as shown in Figure 12.[47]

All studied PILs in this work are conforming to the Walden rule. Indeed, they lie significantly closer to the ideal line with unit slope than aprotic ILs such as quaternary ammonium tetrafluoroborate.[20] However, being further below the "ideal line" than other PILs previously studied, they have a less ionic nature. This is probably due to the relatively low ΔpK_a values between Brønsted bases and acids (from 3.9 to 4.6; see Table 2) as notified by Belieres and Angell.[36] [morph][F] lies above [Mmorph][F] and [Emorph][F] and closer to the ideal line. Its relatively higher ionicity could be explained by the largest number of hydrogen bonds by comparison with the two other studied PILs (Table 2).

Figure 12 shows also that [Pyrr][NO$_3$] and [Pyrr][HSO$_4$], studied by our group in a previous work, lie in the upper part of the Walden diagram.[47] This means they are superior conductors in which the Grotthus mechanism for the transport of protons becomes predominant.

Fragility. Fragility is a novel concept applicable to study the behavior of glass-forming liquids. In a simplified picture, it is

Morpholinium Based Protic Ionic Liquids

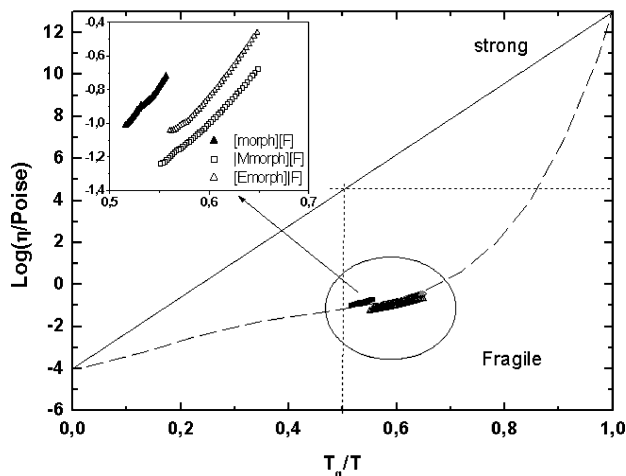*J. Phys. Chem. B, Vol. 114, No. 5, 2010* **1765**

Figure 13. Fragility plot of the three PILs studied in this paper.

associated with the profile of the potential energy surface, increasing with the mean amplitude and variance of the activation barriers. Several approaches have been made to quantify fragility in glassy state physics.[76,77] A plot of $\log(\eta)$ versus the scaled temperature (T_g/T) is more useful in order to visualize and compare fluid fragilities. Angell[78] has classified glass-forming liquids as "strong" and "fragile" on the basis of such a plot. Arrhenius liquids are described as strong, while those following the VTF equation are fragile. Fragility itself has been quantified in various ways.

(i) Fragility (F) as $F = 1/B$,[67] where B is an exponent parameter in the VTF equation (eq 2).

(ii) Fragility (F) as the ratio $F = T_0/T_g$, where T_0 and T_g are the "ideal" glass transition temperature and the glass transition temperature, respectively. This ratio conveniently lies between 0 (strong) and 1 (fragile).[79,80]

(iii) Fragility $F_{kin,1/2}$ (different from F fragility) is given by $F_{kin,1/2} = 2(T_g/T_{1/2})$, where $T_{1/2}$ is the temperature at which $\log \eta$ is half of the above range (see Figure 13).[81]

In this paper, the last relation (iii) is adopted for the fragility determination. The data for present PILs are plotted in Figure 13. The fragility index parameters $F_{kin,1/2}$ (relation in (iii)) obtained are close to $T_g/T_{1/2} = 0.86$ for all samples. It can be seen that morpholinium formate PILs are extremely fragile, similar to extremely fragile salts described by Angell and Belieres, such as the mixture (0.6 KNO$_3$, 0.4 Ca(NO$_3$)$_2$) presenting $T_g/T_{1/2} = 0.82$ and $F_{kin,1/2} = 0.64$.[36] This extreme fragility was also observed in our previous work for pyrrolidinium formate $T_g/T_{1/2} = 0.87$ and $F_{kin,1/2} = 0.74$.[47]

4. Conclusion

Morpholinium and two *N*-alkylmorpholinium formates have been prepared by neutralization of formic acid by the corresponding base. All compounds are liquid at ambient temperature and hence belong to the protonic ionic liquid (PIL) family. Owing to the formation of strong hydrogen bonds between ions of opposite charge, the physical properties of these compounds are strongly sensitive to the length of the alkyl chain on the morpholinium cation. Restricted Hartree−Fock calculations show that [morph][F], [Mmorph][F], and [Emorph][F] present, respectively, three, two, and one hydrogen bond between anion and cation. Owing to the localization of the partial charges on the N-atom of the morpholinium cation and the O-atom of the formate anion, strong Coulombic interactions are also expected, which are able to stabilize these ionic liquids. The molar volume

of these PILs increases with the size of the substituent on the N-atom of the cation, leading to a less compact structure in the liquid state. Transport properties measurements show that the viscosity increases with both the number of hydrogen bonds between ions and the size of the cation and, as a consequence, the specific conductivity decreases. At low temperatures, these PILs form glasses ($T_g = -84$ to -86 °C) which are able to undergo a cold crystallization when reheated to the ambient temperature. These viscous liquids exhibit a Newtonian behavior and a temperature dependence which can be described by the VTF equation using the glass transition temperature determined by DSC measurements as a parameter. As expected from glass-forming liquids, these liquids are fragile, meaning that their properties are strongly dependent on the temperature close to the glass transition. These PILs have good ionic conductivities as compared to organic electrolytes but are less conducting than concentrated aqueous electrolytes. Nevertheless, they have a larger domain of use in temperature as liquid electrolytes than aqueous media: from −15 °C to, at least, +100 °C. They can also be mixed with water in all proportions, and the result is a drastic increase in conductivity. The electrochemical window at the vitreous carbon electrode reaches 2.9 V in the case of [morph][F] but is restricted to about 2.2 V for the two *N*-alkyl substituted compounds.

As a conclusion, this family of ionic liquids can be used as valuable electrolytes owing to their tunable physicochemical and transport properties. In addition, they can be produced easily in large economic scale for a wide range of electrochemical applications.

References and Notes

(1) Wilkes, J. S. *Green Chem.* **2002**, *4*, 73.
(2) Wasserscheid, P.; Keim, W. *Angew. Chem., Int. Ed.* **2000**, *39*, 3772.
(3) Welton, T. *Chem. Rev.* **1999**, *99*, 2071.
(4) Dupont, J.; De Souza, R. F.; Suarez, P. A. Z. *Chem. Rev.* **2002**, *102*, 3667.
(5) Hagiwara, R.; Ito, Y. *J. Fluorine Chem.* **2000**, *105*, 221.
(6) Araos, M. U.; Warr, G. G. *Langmuir* **2008**, *24*, 9354.
(7) He, Y.; Li, Z.; Simone, P.; Lodge, T. P. *J. Am. Chem. Soc.* **2006**, *128*, 2745.
(8) Eastoe, J.; Gold, S.; Rogers, S. E.; Paul, A.; Welton, T.; Heenan, R. K.; Grillo, I. *J. Am. Chem. Soc.* **2005**, *127*, 7302.
(9) Blanchard, L. A.; Hancu, D.; Beckman, E. J.; Brennecke, J. F. *Nature* **1999**, *399*, 28.
(10) Geldbach, T. J.; Dyson, P. J. *J. Am. Chem. Soc.* **2004**, *126*, 8114.
(11) Kim, K.-S.; Shin, B.-K.; Lee, H.; Ziegler, F. *Fluid Phase Equilib.* **2004**, *218*, 215.
(12) Kim, K.-S.; Shin, B.-K.; Lee, H. *Korean J. Chem. Eng.* **2004**, *21*, 1010.
(13) Marsh, K. N.; Deev, A.; Wu, A. C.-T.; Tran, E.; Klamt, A. *Korean J. Chem. Eng.* **2002**, *19*, 357.
(14) Kim, K.-S.; Park, S.-Y.; Choi, S.; Lee, H. *J. Chem. Eng. Data* **2004**, *49*, 1550.
(15) Demberelnyamba, D.; Kim, K.-S.; Choi, S.; Park, S.-Y.; Lee, H.; Kim, C.-J.; Yoo, I.-D. *Bioorg. Med. Chem.* **2004**, *12*, 853.
(16) Kim, K.-S.; Demberelnyamba, D.; Lee, H. *Langmuir* **2004**, *20*, 556.
(17) Seddon, K. R. *J. Chem. Technol. Biotechnol.* **1997**, *68*, 351.
(18) Shah, J. K.; Brennecke, J. F.; Maginn, E. J. *Green Chem.* **2002**, *4*, 112.
(19) MacFarlane, D. R.; Huang, J.; Forsyth, M. *Nature* **1999**, *402*, 792.
(20) Bonhote, P.; Dias, A.-P.; Papageorgiou, N.; Kalyanasundaram, K.; Grätzel, M. *Inorg. Chem.* **1996**, *35*, 1168.
(21) Quinn, B. M.; Ding, Z.; Moulton, R.; Bard, A. J. *Langmuir* **2002**, *18*, 1734.
(22) Sun, J.; Forsyth, M.; MacFarlane, D. R. *J. Phys. Chem. B* **1998**, *102*, 8858.
(23) Kim, K.-S.; Choi, S.; Demberelnyamba, D.; Lee, H.; Oh, J.; Lee, B.-B.; Mun, S.-J. *Chem. Commun.* **2004**, 828.
(24) Greaves, T. L.; Drummond, C. J. *Chem. Rev.* **2008**, *108*, 206.

(25) Greaves, T. L.; Weerawardena, A.; Fong, C.; Krodkiewska, I.; Drummond, C. J. *J. Phys. Chem. B* **2006**, *110*, 22479.

(26) Evans, D. F.; Chen, S.-H.; Schriver, G. W.; Arnett, E. M. *J. Am. Chem. Soc.* **1981**, *103*, 481.

(27) Atkin, R.; Warr, G. G. *J. Am. Chem. Soc.* **2005**, *127*, 11940.

(28) Greaves, T. L.; Weerawardena, A.; Fong, C.; Drummond, C. J. *J. Phys. Chem. B* **2007**, *111*, 4082.

(29) Atkin, R.; Warr, G. G. *J. Phys. Chem. B* **2007**, *111*, 9309.

(30) Evans, D. F.; Kaler, E. W.; Benton, W. J. *J. Phys. Chem.* **1983**, *87*, 533.

(31) Evans, D. F.; Yamauchi, A.; Roman, R.; Casassa, E. Z. *J. Colloid Interface Sci.* **1982**, *88*, 89.

(32) Evans, D. F.; Yamauchi, A.; Wei, G. J.; Bloomfield, V. A. *J. Phys. Chem.* **1983**, *87*, 3537.

(33) Greaves, T. L.; Weerawardena, A.; Fong, C.; Drummond, C. J. *Langmuir* **2007**, *23*, 402.

(34) Triolo, A.; Russina, O.; Fazio, B.; Triolo, R.; Di Cola, E. *Chem. Phys. Lett.* **2008**, *457*, 362.

(35) Atkin, R.; Warr, G. G. *J. Phys. Chem. C* **2007**, *111*, 5162.

(36) Belieres, J.-P.; Angell, C. A. *J. Phys. Chem. B* **2007**, *111*, 4926.

(37) Szklarz, P.; Owczarek, M.; Bator, G.; Lis, T.; Gatner, K.; Jakubas, R. *J. Mol. Struct.* **2009**, *929*, 48.

(38) Lava, K.; Binnemans, K.; Cardinaels, T. *J. Phys. Chem. B* **2009**, *113*, 9506.

(39) Huang, B.; Li, Z.; Shi, N.; Xu, X.; Zhang, K.; Fang, Y. *Youji Huaxue* **2009**, *29*, 770.

(40) Choudhary, A.; Agarwal, S.; Sharma, V. *Indian J. Chem., Sect. A: Inorg., Bio-inorg., Phys., Theor. Anal. Chem.* **2009**, *48A*, 362.

(41) Bodesheim, G.; Schmidt-Amelunxen, M.; Sohn, D.; Grundei, S. 2008, WO 2008154998 A1 20081224.

(42) Wang, J.; Yang, X.; Li, G.; Luan, L. Abstracts of Papers, 237th ACS National Meeting, Salt Lake City, UT, March 22−26, 2009, COLL-238.

(43) Gans, B.-J.; Hansel, R. 2009, US 2009053552 A1 20090226.

(44) Pretti, C.; Chiappe, C.; Baldetti, I.; Brunini, S.; Monni, G.; Intorre, L. *Ecotoxicol. Environ. Saf.* **2009**, *72*, 1170.

(45) Anouti, M.; Caillon-Caravanier, M.; Le Floch, C.; Lemordant, D. *J. Phys. Chem. B* **2008**, *112*, 9406.

(46) Anouti, M.; Caillon-Caravanier, M.; Le Floch, C.; Lemordant, D. *J. Phys. Chem. B* **2008**, *112*, 9412.

(47) Anouti, M.; Caillon-Caravanier, M.; Dridi, Y.; Galiano, H.; Lemordant, D. *J. Phys. Chem. B* **2008**, *112*, 13335.

(48) Sharma, M.; Alderfer, J. L.; Box, H. C. *J. Labelled Compd. Radiopharm.* **1983**, *20*, 1219.

(49) Hirschfelder, J. O.; Curtiss, C. F.; Bird, R. B. *Molecular Theory of Gases and Liquids*; Wiley: London, 1964.

(50) Greaves, T. L.; Weerawardena, A.; Krodkiewska, I.; Drummond, C. J. *J. Phys. Chem. B* **2008**, *112*, 896.

(51) Susan, Md. A. B.; Noda, A.; Mitsushima, S.; Watanabe, M. *Chem. Commun.* **2003**, 938.

(52) Harris, K. R.; Kanakubo, M.; Woolf, L. A. *J. Chem. Eng. Data* **2007**, *52*, 2425.

(53) Tokuda, H.; Tsuzuki, S.; Susan, Md. A. B. H.; Hayamizu, K.; Watanabe, M. *J. Phys. Chem. B* **2006**, *110*, 19593.

(54) Sanmamed, Y. A.; González-Salgado, D.; Troncoso, J.; Cerdeiriña, C. A.; Romaní, L. *Fluid Phase Equilib.* **2007**, *252*, 96.

(55) Pereiro, A. B.; Legido, J. L.; Rodríguez, A. *J. Chem. Thermodyn.* **2007**, *39*, 1168.

(56) Okoturo, O. O.; Vander Noot, T. J. *J. Electroanal. Chem.* **2004**, *568*, 167.

(57) McFarlane, D. R.; Sun, J.; Golding, J.; Meakin, P.; Forsyth, M. *Electrochim. Acta* **2000**, *45*, 1271.

(58) Tao, G.-H.; He, L.; Sun, N.; Kou, Y. *Chem. Commun.* **2005**, 3562.

(59) Galiński, M.; Lewandowski, A.; Stepniak, I. *Electrochim. Acta* **2006**, *51*, 5567.

(60) MacFarlane, D. R.; Pringle, J. M.; Johansson, K. M.; Forsyth, S. A.; Forsyth, M. *Chem. Commun.* **2006**, 1905.

(61) MacFarlane, D. R.; Meakin, P.; Sun, J.; Amini, N.; Forsyth, M. *J. Phys. Chem. B* **1999**, *103*, 4164.

(62) Tsierkezos, N. G.; Philippopoulos, A. I. *Fluid Phase Equilib.* **2009**, *277*, 20.

(63) Zhao, C.; Burrell, G.; Torriero, A. A. J.; Separovic, F.; Dunlop, N. F.; MacFarlane, D. R.; Bond, A. M. *J. Phys. Chem. B* **2008**, *112*, 6923.

(64) Gritzner, G.; Kuta, J. *Pure Appl. Chem.* **1982**, *54*, 1527.

(65) Gritzner, G.; Kuta, J. *Pure Appl. Chem.* **1984**, *56*, 461.

(66) Shiddiky, M. J. A.; Torriero, A. A. J.; Zhao, C.; Burgar, I.; Kennedy, G.; Bond, A. M. *J. Am. Chem. Soc.* **2009**, *131*, 7976.

(67) Suarez, P. A. Z.; Consorti, C. S.; de Souza, R. F.; Dupont, J.; Gonçalves, R. S. *J. Braz. Chem. Soc.* **2002**, *13*, 106.

(68) Suarez, P. A. Z.; Selbach, V. M.; Dullius, J. E. L.; Einloft, S.; Piatnicki, C. M. S.; Azambuja, D. S.; de Souza, R. F.; Dupont, J. *Electrochim. Acta* **1997**, *42*, 2533.

(69) Zein El Abedin, S.; Borissenko, N.; Endres, F. *Electrochem. Commun.* **2004**, *6*, 510.

(70) Andrieux, C. P.; Gonzalez, F.; Savéant, J.-M. *J. Electroanal. Chem.* **2001**, *498*, 171.

(71) Noda, A.; Susan, Md. A. B. H.; Kudo, K.; Mitsushima, S.; Hayamizu, K.; Watanabe, M. *J. Phys. Chem. B* **2003**, *107*, 4024.

(72) Van Valkenburg, M. E.; Vaughn, R. L.; Williams, M.; Wilkes, J. S. *Thermochim. Acta* **2005**, *425*, 181.

(73) Walden, P. Z. *Phys. Chem.* **1906**, *55*, 207.

(74) Yoshizawa, M.; Xu, W.; Angell, C. A. *J. Am. Chem. Soc.* **2003**, *125*, 15411.

(75) Xu, W.; Cooper, E. I.; Angell, C. A. *J. Phys. Chem. B* **2003**, *107*, 6170.

(76) Ediger, M. D.; Angell, C. A.; Nagel, S. R. *J. Phys. Chem.* **1996**, *100*, 13200.

(77) Angell, C. A.; MacFarlane, D. R.; Oguni, M. *Ann. N. Y. Acad. Sci.* **1986**, *484*, 241.

(78) Angell, C. A. *J. Phys. Chem. Solids* **1988**, *49*, 863.

(79) Donth, E. *J. Non-Cryst. Solids* **1982**, *53*, 325.

(80) Hodge, I. M. *J. Non-Cryst. Solids* **1996**, *202*, 164.

(81) Richert, R.; Angell, C. A. *J. Chem. Phys.* **1998**, *108*, 9016.